Physica D 38 (1989) 16–28
North-Holland, Amsterdam

ORDERED SHAPES IN NONEQUILIBRIUM GROWTH

Eshel BEN-JACOB and Peter GARIK
Department of Physics, University of Michigan, Ann Arbor, MI 48109, USA
and School of Physics and Astronomy, Tel Aviv University, 69978 Tel Aviv, Israel

Patterns observed during nonequilibrium growth display complex ordering on many length scales. We focus on ordered patterns which reflect the interplay of microscopic and macroscopic dynamics. The fundamental morphologies which result, and which are the building blocks of more complex patterns, include dendritic and tip-splitting growth. The latter gives rise to the two-dimensional dense-branching morphology (DBM). We review the current understanding of how dendritic growth and the DBM arise from the microscopic dynamics of surface tension and surface kinetics. We emphasize the open questions, with particular attention to the question of developing theory for morphology selection and transitions between dendritic and dense-branching growth. In this context, we review our hypotheses of the selection of the fastest growing morphology, and the existence of first- and second-order-like morphology transitions. Theoretical issues are illustrated using the Hele-Shaw and electrodeposition experiments.

1. Introduction

We are surrounded by a nature out of equilibrium, a nature which presents the scientist with a bewildering and mesmerizing universe of patterns. A principal challenge to physicists is to understand the geometry of these nonequilibrium patterns, whether they arise as physical objects – mountains, snowflakes, dust motes – or as mathematical abstractions, e.g. time correlations, or density fluctuations. The quantification of the geometrical properties of these nonequilibrium systems, and our understanding of the dynamics which gives rise to these geometries, has made large gains over the past decade. In large part this has followed from a recognition that nature supercedes Euclid's Elements, and that much of her patterning is best understood with the "fractal" geometry described by Mandelbrot [1].

Concurrent with the scientific community's recognition that nature is not restricted to patterns of Euclidean dimension, these past few years have seen the development of a new understanding of specific patterns that recur during nonequilibrium growth[*]. These patterns, the dendrite and tip-splitting "fingering" growth, appear on system-dependent length scales varying by many orders of magnitude. In effect, they are the short-length-scale building block morphologies from which are composed the more complex patterns visible on larger length scales. While the larger patterns which develop during solidification, aggregation, or condensation still require new insights to explain the global morphology assemblage, significant progress has been made in understanding the determining physics of dendritic and tip-splitting growth, and their interrelationship as fundamental morphologies.

The cornerstone of the recent developments is the recognition of the interplay of microscopic interfacial dynamics with external macroscopic forces in the determination of growth patterns. Most of the research has focused on systems where the macroscopic dynamics are determined by a diffusion field. We now understand that for these systems, the patterns that form, result from competition between the

[*] By 1611 the great astronomer Johannes Kepler [2] was already captivated by the beautiful shapes of snowflakes, which is perhaps the most striking example of pattern formation in inorganic systems. See also ref. [3]. For a review of the previous phase of the research on pattern formation during solidification see ref. [4].

Essays in honour of Benoit B. Mandelbrot
Fractals in Physics – A. Aharony and J. Feder (editors)

diffusion field on the one hand, and the microscopic dynamics of the interface on the other. The patterns may be grouped into a small number of typical "essential shapes" or morphologies, observed in different systems and over many different length scales (from meters to micrometers). These are the faceted [5], dendritic [4], dense-branching [6] and fractal [7,8] [#2] morphologies (see fig. 1). It is the purpose of this short review to provide a perspective on the advances in the field of morphology selection with an emphasis on general principles and the remaining open questions.

2. The selection problem for dendritic growth

The principal mystery in how microscopic dynamics, operative on the scale of angstroms, is amplified to the extent that in a system out of equilibrium it controls the macroscopic shape on a scale of centimeters. From a theoretical perspective herein lies the rub. The natural inclination is to attempt theories of growth emphasizing macroscopic dynamics and relegate the microscopic dynamics to subsequent refinements of theory. Indeed this was how the theory of dendritic growth initially evolved. In 1947 Ivantsov showed [10] that propagating solutions, with a parabolic shape, exist for a solid forming from an undercooled melt by assuming only diffusion control of the heat field but *neglecting surface tension and surface kinetics*. Both the parabolic shape and the predicted constant velocity fit well a semi-quantitative description of a dendrite. However, a conundrum comes with the Ivantsov solution: it specifies only the product of the dendrite tip's radius of curvature and velocity, but cannot predict either one alone. The 1976 experiments of Glicksman et al. [11] demonstrated that under controlled conditions, *for given undercooling* the same dendrite (i.e. same tip velocity and radius of curvature) is reproducibly observed. This implies a "selection problem": for given undercooling the Ivantsov solution admits a continuous family of parabolic solutions, and yet for specified conditions only one is observed. Moreover, it was shown that these Ivantsov solutions were also "linearly unstable", meaning that they would be unable to maintain their shape during growth.

Sensibly the first attempts to resolve the stability problems were based on a hope that incorporation of surface tension would involve only a minor shape modification of Ivantsov's parabolic fronts, while stabilizing all parabolas below a characteristic length scale. However, the selection problem remained inherent in this. In 1973 Oldfield [12] proposed that the selected dendrite was the one moving with the minimum speed (or maximum radius of tip) for which the surface tension can stabilize the underlying needle-crystal. Oldfield's idea was revived and elaborated in 1977 by Langer and Müller-Krumbhaar [13], who performed extensive calculations in order to find this marginally stable operating point.

The real breakthroughs in understanding dendritic growth waited until this decade, and arrived with results of broader significance for morphology determination. The resolution required sufficient computing power and the subsequent application of more advanced mathematical methods, to properly incorporate the microscopic dynamics. The surprise was that despite their small size, surface tension and surface kinetics are singular perturbations in the dynamical equations for interface evolution. Singular perturbations, no matter how small, totally change the character of the solution. As such, the microscopic dynamics cannot be treated as small corrections to solutions initially determined from the macroscopic dynamics. What has emerged is that when surface tension and surface kinetics are isotropic, dendritic growth does not occur. Instead tip-splitting fingers develop leading to the dense-branching morphology. Anisotropy is required in the interfacial dynamics to produce dendritic growth [#3]. This picture is now con-

[#2] For a review of the recent developments in the study of diffusion-limited aggregation (DLA) growth see ref. [9].

[#3] This was first demonstrated in a local model of solidification – the boundary layer model [14].

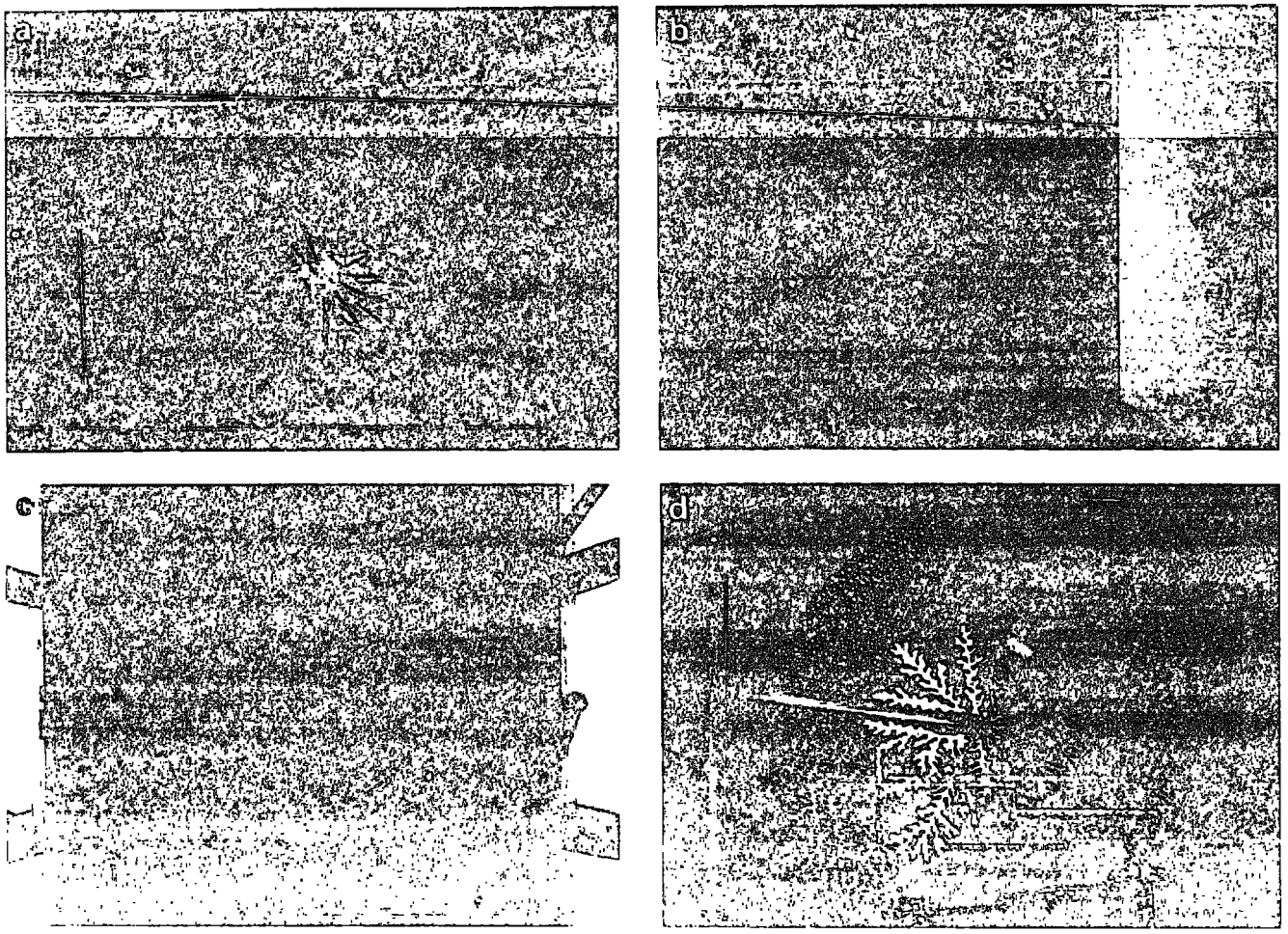

Fig. 1. The "essential shapes" in the Hele-Shaw experiment. As we explain in the text the endless array of shapes can be grouped into a small number of characteristic shapes reflecting significant dominant effects. The same shapes (the geometrical characteristics) are observed in different systems and on different length scales (from meters to micrometers). (a) The dense branching morphology. The characteristic morphology in the absence of crystalline anisotropy can be characterised by the number of branches as function of the radius (the spacing between the branches and the branches' width are the characteristic length scales). Note that it has a well-defined circular envelope. (b,c) Dendrites. As we now understand anisotropy is required for dendritic growth to occur. The dendrites are characterized by a trunk with a parabolic tip moving at constant velocity [4]. The trunk is feathered with side branches which grow outward while being stationary in the laboratory frame. Under some growth conditions sidebranches are observed. We refer to the underlying trunk (the dendrite without the sidebranches) as a needle-crystal. The dendrites have characteristic length scales: the radius of the tip and the spacing between sidebranches. (d) A fractal-like shape [1,7–9]. It is characterized by the fractal dimension (related to the mass distribution as a function of the radius). This is the typical shape in the limit of small surface tension and large noise. It appears similar to the structure produced by the diffusion-limited aggregation (DLA) model [7,8]. (a) A typical example of an air DBM. The applied pressure is about 150 mbar and the spacing between the plates is about 0.4 mm. (b) A typical example of a four-fold "snowflake" in an anisotropic Hele-Shaw cell with a fourfold symmetry. Note the parabolic shape of the tip of each arm and the train of side branches growing out from each one. (c) An example of a "snowflake" in an anisotropic Hele-Shaw cell with a sixfold symmetry. We raised the applied pressure during the growth. This [illegible] occurs when real snowflakes are formed in clouds moving through regimes with different levels of supersaturation. (d) A DLA-like shape developed in the case of large noise and no surface tension. A random array of channels is engraved on the bottom of the square between the plates. The top plate was placed flat on the bottom one. This way the fields in two adjacent channels are not connected, leading to effectively no surface tension.

firmed by both experimental [15,16] and theoretical results [14,17] [4].

New selection problems emerged with the broader understanding of pattern determination. The puzzle is no longer the dendrite's velocity and shape alone. Now the questions are as to why dendrites are selected for some parameters, and tip-splitting growth for others. To study these new selection problems we turn to an experiment in which the interfacial dynamics is expressed on the same length scale as the pattern [15,19,20]. These experiments, discussed below, permit unambiguous demonstration of morphology selection as a function of anisotropy.

3. The dense-branching morphology

To study pattern formation for isotropic interfacial dynamics, we used a modification of the Hele-Shaw cell [5]. This simple, yet elegant, device for studying pattern formation consists of two closely spaced plexiglass plates sandwiching a layer of viscous fluid – here dyed glycerine. The top plate is circular and open to air at its edge. Through an inlet at the center of the top plate a less viscous fluid (e.g. air or water) is injected into the glycerine.

In fig. 1a an example of the dense-branching morphology (DBM) in the cell is shown. It consists of a circular envelope modulated by leading branch tips. The regular tip-splitting of the fingers distinguishes them from dendrites. Moreover, the lacunae or gaps between the fingers do not grow with the area of displaced fluid. This distinguishes the mass distribution of the DBM from that of a fractal object, such as a diffusion-limited aggregate (DLA), where the gaps grow ever larger with the overall size of the pattern. Instead, the DBM grows as a two-dimensional object, although in some cases it may approach $d = 2$ only asymptotically [20].

Experimental evidence supports the conclusion that, in the absence of anisotropy, the DBM is the generic morphology [6,20]. This is contrary to the argument that fractal growth should be the usual *macroscopic* morphological organization [25] [6]. The DBM is observed in aggregate growth by electrochemical deposition [7] and precipitation from supersaturated solution [29]; during solidification from undercoooled melts [30] [8]; arising during amorphous annealing [6]; and in spherulitic growth [31].

Our present understanding of the DBM is based on analyzing its branching rate, as opposed to its mass distribution or coastline. Generally, we expect the branching rate, or surface modulation, to be the result of the interplay between the macroscopic diffusion field, which tends to make the interface irregular, and the microscopic effects of surface tension and surface kinetics. These introduce cutoff lengths and define the length scale of ordered growth. Turning again to the Hele-Shaw example, the governing equations for the pressure field are:

$$\nabla^2 p = 0 \quad \text{(Laplace's equation)},$$

$$p_i = p_{app} - \sigma\kappa \; [illegible] \; v_n$$

(Gibbs–Thomson [illegible]),

$$v_n = \frac{-b^2}{12\eta} \nabla p \cdot \hat{n} \quad \text{(D'Arcy's law)}.$$

Here p_i is the pressure in the fluid at the interface, p_{app} is the pressure applied to the less viscous fluid, σ is the interfacial surface tension, κ is the curvature of the interface, $\hat{n}$ is the unit normal to the interface in the direction of the viscous fluid, [illegible]

[4] For a more mathematical description of the new developments, see ref. [13].

[5] The original Hele-Shaw cell was a long narrow channel containing a fluid sandwiched between two plates. It was used to study the flow of water around a shaped object [illegible]. Variations of the Hele-Shaw cell are very much in current use. See for example, ref. [22] and the review paper by Bensimon et al. [23]. The circular geometry was first employed by Paterson [24].

[6] Following ref. [14], first dendritic growth [illegible] when anisotropic surface tension is included. [illegible] branches would develop [illegible].

[7] The dense-branching morphology was first observed during electrochemical deposition; see for example refs. [27,28].

[8] Fujioka observed dendritic growth in solidification of water at higher undercooling and tip-splitting at low undercooling.

coefficient, b is the spacing between the plates, and η is the fluid viscosity. The exponent γ has been computed as $\frac{1}{2}$ for a uniform wetting layer, would be different for a non-Newtonian fluid, and is taken as unity in our simple analysis below. Although the differential equation for the pressure field here is Laplace's, the physics of these equations is nearly isomorphic to problems where the governing equation is strictly the diffusion equation, e.g., precipitation from supersaturated solution, or solidification from an undercooled melt.

Linear stability analysis [32] [*] can be used to investigate the branching rate of the DBM. Indeed, the instability of a diffusion-controlled interface to any perturbation in the absence of a Gibbs–Thomson-like stabilization, is the Mullins–Sekerka instability. Using the above equations, we can compute the relative growth rate of perturbations on a disk of radius R. Taking the perturbation to be of the form $r(\theta)=R+\delta_m\cos(m\theta)$ for small δ we find that:

$$\alpha_m(\lambda)\equiv\frac{\dot{\delta}_m/\delta_m}{\dot{R}/R}$$

$$=-1+m\left(\lambda+\tilde{\beta}-\frac{(m^2-1)(\lambda^{1-\gamma}-\lambda^{-1}+\tilde{\beta})}{\xi\lambda-1}\right)$$

$$\times\left[m\tilde{\beta}+\lambda\left(\frac{1-\lambda^{-2m}}{1+\lambda^{-2m}}\right)\right]^{-1},$$

where

$$\xi=\frac{p_\infty-p_0}{d_0/R_0},$$

$$\tilde{\beta}=\beta b^2/12\eta R_0,$$

and

$$\lambda=R/R_0,$$

R_0 the cell radius. Fig. 2 shows that there is a fastest growing perturbation. Experimentally, good agreement is found between this fast growing mode and the number of branches as a function of radius [6,34]. This analysis is consistent with the DLA-like dimension of mass of small Hele-Shaw patterns; however, the branching rate increases with λ such that past a critical value, determined by system parameters, the growth is $d=2$ as observed visually [20].

In the absence of stabilizing effects at the interface, such as surface tension or surface kinetics, the diffu-

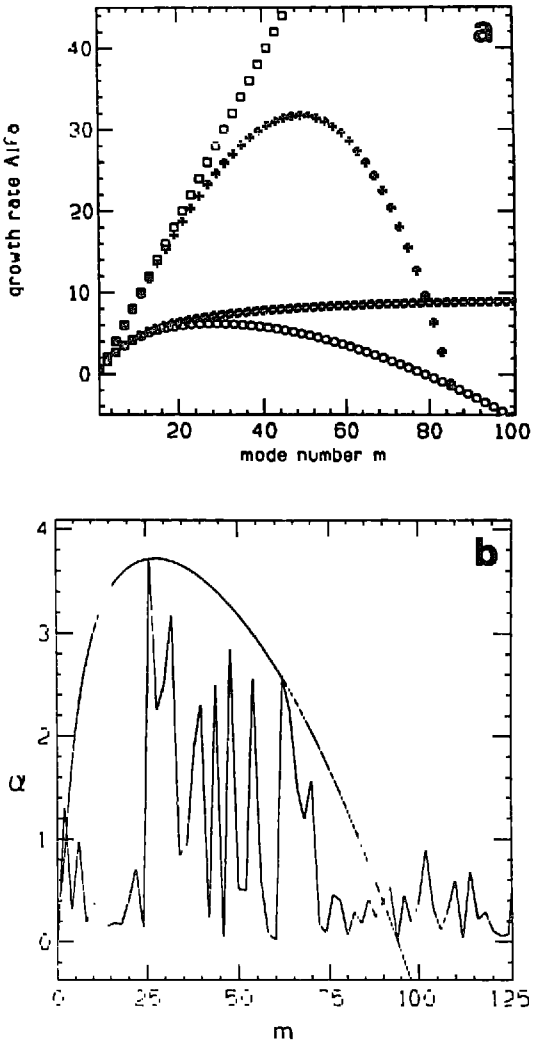

Fig. 2 The DBM and the linear stability analysis (a) Results of the linear stability analysis, showing the initial growth rate as function of the mode number m for a sinusoidal perturbation d of a circular interface. Line (1) is for constant pressure along the interface (no surface tension and no surface kinetic), line (2) is when surface tension is included and line (3) is in the presence of surface kinetics. Note that in the latter case there is no fastest growing mode. Line (4) is in the presence of both surface tension and surface kinetic. (b) shows a comparison of the linear stability and an experimental power spectrum of the envelope of a DBM developed in the Hele-Shaw cell. See ref. [20] for more details.

[*] A similar linear analysis to that presented here was performed independently by Schwarz [33].

sive Mullins–Sekerka instability results in an unstable interface. The result is noisy, apparently fractal, growth. This is what happens in the modelling of growth by the DLA algorithm [7,9], where there is no surface tension. This is also the case when two miscible fluids are used [35], or glass beads are added [36], in fluid flow experiments. In both of these cases the net result is to reduce the interfacial stabilization effect of surface tension.

The nature of the envelope of the DBM is an integral part of the dynamics of the pattern but its understanding requires a nonlinear analysis [10]. A naive understanding is that if one finger outgrows the others, it has more space to spread out; part of the flow goes sideways and the finger flattens and slows down. In our view, the most pressing unsolved problem is to understand the branching rates and velocity of DBM growth [19,31]. The latter is especially intriguing because there may be a selection mechanism operating with respect to the branching rate and interfacial velocity akin to the tip-radius and velocity of the dendrite selection problem [38].

4. Dendritic growth and morphology diagram in the anisotropic Hele-Shaw cell

The Hele-Shaw cell can also be used to study anisotropic growth, analogous to the solidification of a crystalline material. There is a strikingly simple way to mimic crystalline anisotropy in the fluid cell: one engraves channels on one of the plates. The channels modulate the spacing between the plates so as to create deep and shallow paths for the flow of fluid. When the grooved lattice has six-fold symmetry (three sets of parallel channels oriented at 120° to each other), the air bubble adopts beautiful snowflake-like shapes with six dendritic arms. Since snowfall on Mars is composed of CO_2 flakes with fourfold anisotropy, a fourfold lattice produces the "Martian snowflakes" of fig. 1b. The emergence of dendrites in the Hele-Shaw cell [15] provided the first direct experimental demonstration that anisotropy is needed for dendritic growth to occur.

But not only dendritic growth is observed in the presence of anisotropy. As we vary the applied pressure (the driving force) the air bubble assumes different shapes. Similarly, different morphologies are observed as the "microscopic" growth conditions are changed. For example, we can change the level of anisotropy simply by changing the spacing between the plates. The idea of a "morphology diagram" to organize the observations follows naturally [19, 20].

Fig. 3 depicts a morphology diagram for a cell with sixfold anisotropy. Faceted growth, the DBM, and *two types* of dendrites now occur, for different values of the applied pressure. As we will see later on, the existence of two types of dendrites play an important role in our understanding of morphology transitions. A morphology diagram is also observed in electrochemical deposition experiments [27,28], Hele-Shaw cells using liquid crystals as the viscous fluid [16], and solidification from supersaturated solutions [39].

Several questions arise now: why does anisotropy trigger dendritic growth, and if it does, why is the DBM still observed? Why do some dendrites appear when the system is driven far from equilibrium, but different ones appear close to equilibrium? Is there a general selection principle that will determine which growth will be observed for specified conditions, leading to a theoretical understanding of morphology diagrams?

5. Anisotropy and the formation of dendrites

The first understanding and clear demonstration of the singular nature of microscopic effects, and the need for anisotropy for dendritic growth, emerged from the study of two simple models of interfacial growth [14,17]. The immediate goal in the construction of these models was to pinpoint the physical effects that were essential for dendritic growth. Earlier attempts without the drastic simplifications of the lo-

[10] In ref. [37] it is claimed that the circularity of the envelope in electrochemical deposition can be explained solely on the basis of linear stability analysis when the aggregate has a finite resistivity.

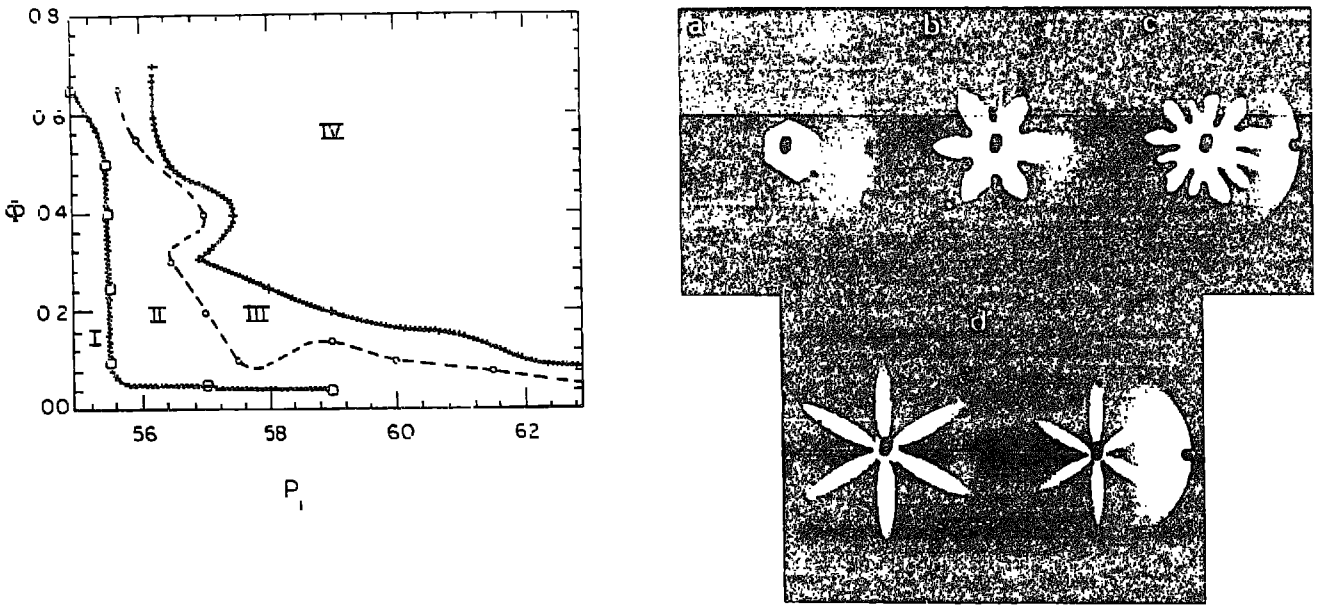

Fig 3 Morphology diagram for a sixfold anisotropic Hele-Shaw cell (the cell is the same as described in refs. [15.19].) Here P_1 is the applied pressure measured roughly in centimeters of Hg (the actual manometer fluid was a light oil). The anisotropy of the cell is measured by the ratio $\Phi=b_1/(b_0+b_1)$, where b_1 is the depth of the grooves (0.015 in) and b_0 is the additional spacing between the top plate and the top of the grooved plate. The morphology regions are (I) faceted growth; (II) surface-tension dendritic growth (with careful inspection it is possible to observe that the dendrites point at an angle of 30° to the ruling of the grooves); (III) tip splitting growth; (IV) kinetic dendritic growth. The needle crystals grow parallel to the ruled channels. Cross hatching of curves separating labelled morphology regions indicates the possible existence of narrow regions of other morphologies, e.g. between regions I and II there is evidence for DBM growth. The dendrites pointing at 30° from the channels occur at lower pressure, for which surface tension is the crucial factor, hence the name "surface tension dendrites". In the directions of the tips of the dendrites the change in interfacial energy when moving the interface is smaller, making it easier to bend the interface. The effective surface tension is weaker and the surface tension anisotropy "prefers" these directions. At higher pressure the surface kinetics dominates, "preferring" dendrites that point along the channels [19] as the relative wetting effects are smaller and the velocity (for the same pressure gradient) is higher. Hence the name "surface kinetic dendrites". In the dividing regime the two effects (surface tension and surface kinetics anisotropy) are of comparable strength and cancel each other, leading to vanishing effective anisotropy and hence a DBM growth. There are additional details not presented in the morphology diagram. For example as the pressure is increased kinetic dendrites with different structure of sidebranches are observed. Only the main features of the morphology diagram are presented here. (a)–(d) are faceted, surface tension dendrites, DBM and surface kinetic dendrites, respectively.

cal models had failed because of the difficulty of solving even numerically the full diffusion problem. In the local models, the interface is treated as a dynamical entity (a "string" in two dimensions). Physical arguments are then used to deduce its equation of motion so as to include microscopic effects at the interface. One such model, the boundary-layer model (BLM), was inspired by solidification from an undercooled melt [14]. In this model the diffusion field is represented by a boundary layer around the string. The great advantage in adopting such a local model is the numerical tractability. This allows a time-dependent solution on the computer explicitly showing the interfacial evolution. In this way it was first recognized that in the absence of anisotropy tip-splitting growth occurs and that anisotropy is necessary for stable dendrite evolution. This latter observation was first considered to be an artifact of the boundary-layer model and not a reflection of universal behavior. Only after the demonstration of the anisotropic Hele-Shaw experiment was the role of anisotropy widely accepted.

A heuristic argument can be provided to explain the role of anisotropy in "shielding and selecting"

the dendrite's tip. Consider a parabola of the form $y=-ax^2$. Let θ be the angle between a surface normal and the y-axis direction. The simplest way to introduce anisotropy is in the surface tension $d(\theta)$ where the angular dependence is presumed to arise from variations of surface tension with different crystallographic orientations. Explicitly we write the Gibbs–Thomson relationship relating the surface temperature T_s and the melting temperature T_M:

$$T_s = T_M - d(\theta)\,\kappa$$

and

$$d(\theta) = d_0[1 - d_1\cos(6\theta)]$$

for the case of sixfold symmetry. First consider the case of no anisotropy, $d_1=0$. Then the tip, $\theta=0$, is the coldest point on the interface. As such it experiences the maximum temperature gradient and is the fastest growing point on the interface. The dynamic response of the system to this circumstance must be diffusion of heat along the interface toward the tip. This will cause the tip to slow down. We further reason that symmetrically placed points can develop on the interface which grow more rapidly than the tip. The result is a splitting of the tip as these other points overwhelm it. To avoid this scenario and permit a stable tip heat flow towards the tip must be suppressed. This is exactly the effect provided by crystalline anisotropy[41]. With anisotropy the coldest point moves away from the tip to a point with a different growth direction. For large enough anisotropy (of the order of a percent or so), this will lead to a rather subtle interplay of the anisotropy and the possible needle-crystal. For a given anisotropy only the needle-crystal with the right tip velocity and tip curvature will feature the coldest point at the right temperature and the right distance from the tip (in terms of arclength) to exactly balance the original tip-splitting dynamics. The result is, instead of the original (Ivantsov) continuous family of parabolas only a discrete set of needle-crystal solutions (with close to parabolic shapes) can satisfy the subtle interplay giving rise to a "solvability" criterion.

This argument motivates the role provided by anisotropy in the existence of stable steady-state needle-crystal-like solutions. But, how does this lead to dendritic growth composed of a needle-crystal trunk decorated with side-branches, *and the selection of a specific dendrite*? If we perturb the needle-crystals, say by introducing a bulge near the tip, the perturbation will grow according to the diffusive instability referred to above. The bulge will grow outward at a fixed position in space, so as the tip advances, the perturbation moves backward if viewed from the tip. It can be imagined that only for the fastest needle-crystal will the bulge move backward faster than its growth rate, allowing the tip to restore its shape despite the growing perturbation. This mechanism results in decorating the *fastest* needle-crystal with side branches, and turning it into the observed dendrite, the only one that can exist.

The numerical formulation of this "microscopic solvability" criterion was discovered independently in 1984 with both the geometrical [41] and the boundary-layer models [42]. Moreover, despite the hand-waving nature of the arguments above, it has since been shown that of the discrete set of possible needle-crystals only the fastest is linearly stable. By now it is known that the same mechanism is present in the full solidification problem [43], and for Hele-Shaw in a channel geometry. This latter is known as the Saffman–Taylor problem with the channel walls providing the necessary anisotropy for selection [44]. Most recently analytic methods have been developed to compute the selected velocity in the limit of small undercooling and small anisotropy [45]. Additional support for the selection principles is provided by comparison with recent time-dependent computer simulations of the full solidification problem [46]. [illegible] by comparison with experiments. Although the preliminary results are promising [47], much more study is required.

A remaining question is the nature of side-branching during dendritic growth. Much attention is given

[41] Other means of anisotropy can also lead to the formation of needles, see for example ref. [40].

to this question now [48], with the debate focusing on the relative role of noise as opposed to deterministic dynamics in the growth of side branches. Either they emerge as a result of noise that excites the diffusive instability and linear stability is sufficient to predict their evolution, or an additional solvability principle is required. We believe the latter to be the case; however, we must leave this topic outside the scope of the present article.

6. The "fastest growing morphology" selection hypothesis and the morphology diagram

Despite the discovery of the microscopic solvability criterion, the problem of dendritic growth is not fully resolved [49]. Time-evolution studies of the interface in the boundary-layer model, and the anisotropic Hele-Shaw experiment, present a nagging problem. Both show that even with anisotropy present, dendrites are not always observed. As we decrease the driving force (pressure in the Hele-Shaw cell and undercooling in the BLM) there is a critical value below which dendritic growth is no longer observed, instead tip-splitting (the DBM) occurs. Similar behavior is also observed during freezing of water [30]. These results contradict the selection principle for dendritic growth, which suggests that as long as anisotropy is present, a specific dendrite (corresponding to the fastest needle-crystal) can exist and is linearly stable. The observation of the DBM under growth conditions suitable for dendrites as well means that with present theory the two morphologies can coexist. "Microscopic solvability" can clearly be only part of the picture. A more general principle is needed to distinguish between different morphologies and determine the one which is selected.

We have proposed [19] the more general principle that *it is the fastest growing morphology which is the dynamically selected one*. That is, if more than one morphology is possible, only the fastest one is nonlinearly stable and will be observed. Thus, one might infer that below some critical driving force the velocity of the DBM is higher than that of dendritic growth, and so the former is selected. Motivated by our Hele-Shaw experiment we have also studied the case of competing anisotropies. Both surface tension and surface kinetic anisotropies are included and they have preferred growth directions offset by 30° as in the sixfold Hele-Shaw cell. We calculated the selected velocity both along the surface tension and the surface kinetic directions. The results (fig. 4) show that above a critical undercooling Δ_c both types of dendrites are possible, with the surface kinetic ones having the higher velocity. Time-dependent simulations of the BLM demonstrate that indeed the surface kinetic dendrites are the dynamically selected morphology in this regime.

Let us explore further the analogy between phase and morphology diagrams. For phases in equilibrium, for a given set of conditions the phase that minimizes the free energy is the selected one, independent of the prior history of the system; the concepts of a selection principle and a phase diagram go hand in hand. In contrast, nonequilibrium growth processes are time dependent, so it is not clear a priori that a morphology diagram should exist (that is, that the shape will depend only upon the growth conditions and not on the history). However, if it does exist, a selection principle must exist if a given morphology is reproducible for a given set of growth conditions. Given such a morphology selection principle, it is possible to generate a map of what shapes should be observed for what growth conditions. The existence of a morphology diagram has been confirmed experimentally in various systems, suggesting that a selection principle must exist. Is this principle the "fastest growing morphology" hypothesis that we have proposed? We believe that the latter is not the most general principle we seek, but is a step in the right direction.

When a system is driven out of equilibrium by the imposition of a gradient in one of the thermodynamic variables (e.g. the temperature or the concentration), the response of the system is described by the conjugate flux (the heat flux and particle flux, respectively). These fluxes may in general be viewed as the rate of entropy production, or the rate of ap-

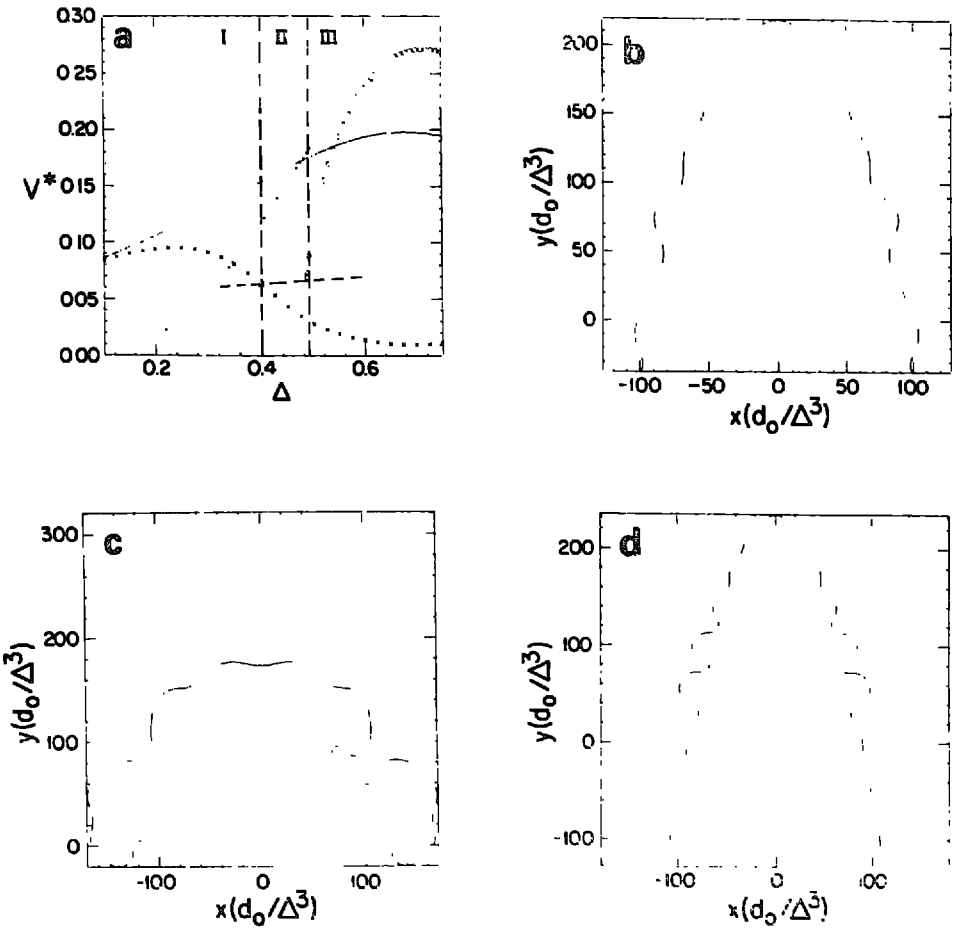

Fig 4 (a) The morphology diagram and the needle-crystal selected velocity v^* (in the dimensionless units of refs [15–20]) for competing anisotropies in the BLM. Both surface tension and surface kinetics anisotropies are included and they have preferred growth directions offset by 30° as in the sixfold Hele-Shaw cell. We have calculated the selected velocity of both the needle-crystals pointing in the preferred direction of the surface tension anisotropy (the crosses) and of those pointing in the surface kinetic preferred direction (diamonds), for more details see ref. [19]. The dashed lines represent our expectation of the DBM velocity. The insets show results of the time-dependent simulations in the three regimes of the morphology diagram. (I) "Surface tension" dendrites (pointing in the surface tension preferred growth directions). (II) tip-splitting, and (III) surface kinetic dendrites. In regime II the two anisotropies are close in effective strength (when acting alone, the two lead to dendrites with similar velocities as is discussed in ref. [19]). The result is a dramatic decline in the selected velocity of the surface tension dendrites, the disappearance of the surface kinetic ones and the appearance of tip-splitting. Above Δ_1 the surface kinetic dendrites have the higher velocity and are the observed morphology. There is a jump in the velocity at Δ_1 hence the DBM–surface kinetic dendrites is a first-order transition. The surface tension–DBM is a second-order change in the slope of the velocity as function of Δ. (b), (c) and (d) are examples of time evolutions in regimes I, II and III respectively.

proach towards global equilibrium. In growth processes, specifically, the driving force (e.g. the undercooling in solidification) is the equivalent of the thermodynamic gradient. The average velocity measures the rate of approach towards equilibrium, and serves naturally as a response function. But the global rate of change of the free energy (at the interface) is given by the integral of the velocity along the interface. Thus, by the term "average velocity" we mean the velocity weighted according to the geometry of the interface, and thus take into account the global shape of the object. We expect this "average velocity" to be an important variable, but by no means the only one. It should have a counterpart (at present unknown) that will represent the equilibrium properties of the interface and the selected growing phase

The fastest growing morphology is probably a good approximation of the general selection principle far enough from equilibrium, where the rate becomes the more dominant part in the competition. It may be viewed as a high-temperature limit of an equilibrium system coupled to a heat bath where the entropy dominates. In the same way we expect that far from equilibrium the entropy production is dominant in selecting the morphology.

The analogy with equilibrium systems may be carried even further. We have proposed the existence of two types of morphology transitions [19], as we vary the growth conditions, in analogy to phase transitions in equilibrium. The first kind shows a discontinuous jump in the velocity at the transition point (hence classified as a first order morphology transition). In the other type (characterized as second order), the velocity itself is continuous as the morphology changes, but shows discontinuity in its derivative.

In fig. 4 we show an example of both first-order and second-order morphology transitions found in the BLM. Again we wonder: is this a general phenomenon or an artifact of the BLM? Chan et al. have made a careful study of solidification from supersaturated NH_4Cl solutions [39]. In particular, their experimental data include information about the velocity of growth which fits well in the framework of morphology transitions described above. They found that, corresponding to changes in crystallographic orientation of the growing dendrites, there was either a jump discontinuity (first order) or a discontinuity in the slope (second order) of the observed dendritic velocity versus supersaturation.

Experiments in growth by electrochemical deposition also produce results in qualitative agreement with the characterization of morphology transitions advanced here. Sawada et al. [27] have plotted the interfacial velocity versus applied voltage and found sudden changes in slope when the morphology changes. In our own experiments of electrochemical

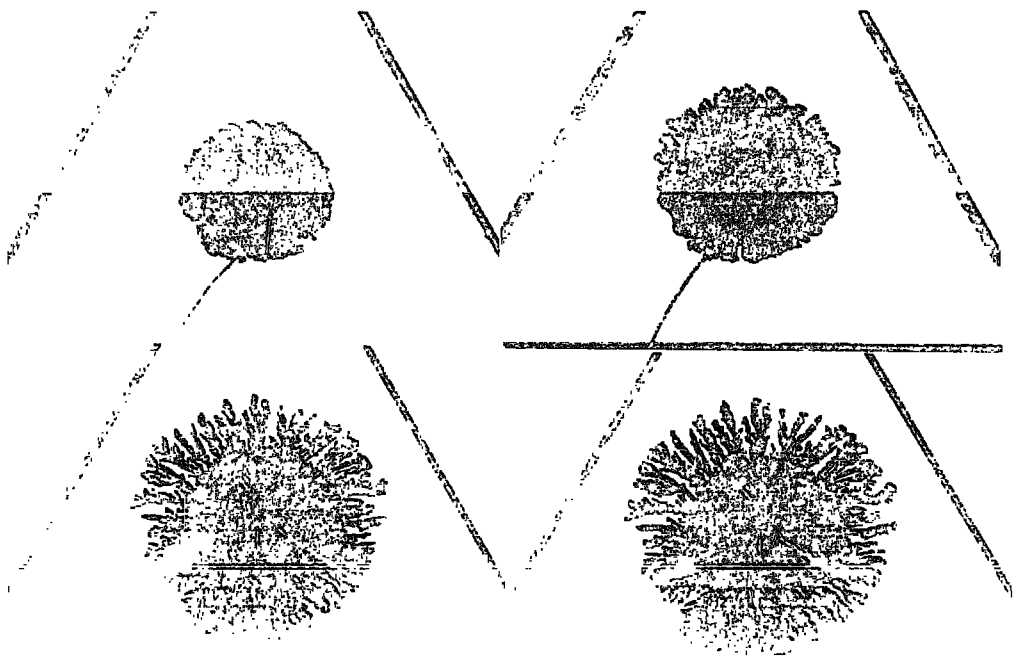

Fig. 8. Morphology transition in electrochemical deposition of Zn from 0.03 M of $ZnSO_4$ solution sandwiched between two plexiglass plates with about 0.3 mm spacing [38]. The outer anode has a triangular shape (8 cm edge). The transition is from tip-splitting growth to dendritic growth. There is also a change in color that reflects the change in the microscopic structure of the two morphologies. Similar transitions between two dense-branching morphologies with different branch density have also been observed in electrochemical deposition of copper [35, 50].

deposition we have observed similar sudden changes in the interfacial velocity with associated morphology transitions [38]. An example of morphology transitions in an electrochemical deposition experiment is shown in fig. 5. It demonstrates two aspects: the sharpness of the transition and a change in the microstructure of the growing deposit (shown as a color change) corresponding to the morphology change. These observations give additional support to the use of morphology transitions nomenclature.

7. Conclusion

The field of nonequilibrium growth has made enormous strides over the past several years. However, many questions remain unanswered. The most pressing is the lack of a theory which can predict morphology selection in diffusion-controlled systems as a function of known control parameters. More general nonequilibrium principles also remain to be resolved, with the question of the nature of morphology transitions one of the most interesting.

Acknowledgements

We are very grateful to Kieran Mullen and Michal Ben-Jacob for their indispensable assistance in preparing and critiquing the manuscript. The research described here was partially supported by grants from: the US National Science Foundation, the Germany–Israel Foundation, and the Donors of the Petroleum Research Fund administered by the American Chemical Society

References

[1] B.B. Mandelbrot, Fractals: Form, Chance and Dimension (Freeman, San Francisco, 1977); The Fractal Geometry of Nature (Freeman, San Francisco, 1982).
[2] J. Kepler, De Nive Sexangula Godfrey Tampach, Frankfurt am Main (1611).
[3] D'Arcy Wentworth Thompson, On Growth and Form (Cambridge Univ. Press, Cambridge, 1942).
[4] J.S. Langer, Rev. Mod. Phys. 52 (1980) 1.
[5] D.P. Woodruff, The Solid-Liquid Interface (Cambridge Univ. Press, Cambridge, 1973).
[6] E. Ben-Jacob, G. Deutscher, P. Garik, N.D. Goldenfeld and Y. Lareah, Phys. Rev. Lett. 57 (1986) 1903.
[7] T.A. Witten and L.M. Sander, Phys. Rev. Lett. 47 (1981) 1400, Phys. Rev. B 27 (1983) 5686;
P. Meakin, Phys. Rev. A 27 (1983) 604, 1495.
[8] M. Matsushita, M. Sano, Y. Hayakawa, H. Honjo and Y. Sawada, Phys. Rev. Lett. 53 (1984) 286.
[9] L. Pietronero and E. Tosatti, eds., Fractals in Physics (North-Holland, Amsterdam, 1985);
J. Nittmann and H.E. Stanley, Nature 321 (1986) 663;
L.M. Sander, Nature 322 (1986) 789;
H.E. Stanley and N. Ostrowsky, eds., Random Fluctuations and Pattern Growth: Experiments and Models (Kluwer, Dordrecht, 1988).
[10] G.P. Ivantsov, Dokl. Akad. Nauk. SSSR 58 (1947) 567.
[11] M.E. Glicksman, R.J. Shaefer and J.D. Ayers, Metall. Trans. A 7 (1976) 1747;
S.C. Huang and M.E. Glicksman, Acta Metall. 29 (1981) 701, 717.
[12] W. Oldfield, Mater. Sci. Eng. 11 (1973) 211.
[13] J.S. Langer and H. Muller-Krumbhaar, Acta Metall. 26 (1978) 1681, 1689, 1697.
[14] E. Ben-Jacob, N.D. Goldenfeld, J.S. Langer, and G. Schon, Phys. Rev. Lett. 51 (1983) 1930; Phys. Rev. A 29 (1984) 330.
[15] E. Ben-Jacob, R. Godbey, N.D. Goldenfeld, J. Koplik, H. Levine, T. Muller and L.M. Sander, Phys. Rev. Lett. 55 (1985) 1315.
[16] A. Buka, J. Kertesz and T. Vicsek, Nature 323 (1986) 424; V. Horvath, T. Vicsek and J. Kertesz, Phys. Rev. A 35 (1987) 2353.
[17] R.C. Brower, D. Kessler, J. Koplik and H. Levine, Phys. Rev. Lett. 51 (1983) 1111; Phys. Rev. A 29 (1984) 1335.
[18] D. Kessler, J. Koplik and H. Levine, Adv. Phys. 37 (1988) 255.
[19] E. Ben-Jacob, P. Garik, T. Muller and D. Grier, Phys. Rev. A 38 (1988) 1370.
[20] E. Ben-Jacob, P. Garik and D. Grier, Superlattices Microstructure 3 (1987) 599.
[21] H.S. Hele-Shaw, Nature 58 (1898) 34.
[22] [illegible], Phys. Rev. Lett. 52 (1984) 1033.
[23] E. Ben-Jacob, R. Godbey, N.D. Goldenfeld, J. Koplik, H. Levine, T. Muller and L.M. Sander, Phys. Rev. Lett. 55 (1985) 1315;
C. Tang, Phys. Rev. Lett. 55 (1985) 2617.
[24] L. Paterson, J. Fluid Mech. 113 (1981) 513; Phys. Rev. Lett. 52 (1984) 1621.
[25] S.N. Rauseo, P.D. Barnes Jr. and J.V. Maher, Phys. Rev. A 35 (1987) 1245;
Y. Muller, W. Knorr and H. Wohlrabold, Phys. Rev. Lett. 56 (1986) 2633.

J. Nittmann and H.E. Stanley, Nature 321 (1986) 663.

[26] L.M. Sander, P. Ramanlal and E. Ben-Jacob, Phys. Rev. A 32 (1985) 3160.

[27] Y. Sawada, A. Dougherty and J.P. Gollub, Phys. Rev. Lett. 56 (1986) 1260.

[28] D. Grier, E. Ben-Jacob, R. Clarke and L.M. Sander, Phys. Rev. Lett. 56 (1986) 1264.

[29] E. Raz, E. Polturak and S. Lipson, preprint and private communications.

[30] T. Fujioka, Ph. D. Thesis, Carnegie-Mellon University (1978).

[31] N.D. Goldenfeld, J. Crystal Growth 84 (1987) 601.

[32] W.W. Mullins and R.F. Sekerka, J. Appl. Phys. 34 (1963) 323, 35 (1964) 444.

[33] L. Schwartz, Phys. Fluids 29 (1986) 3086.

[34] A. Buka and P. Palffy-Muhoray, Phys. Rev. A 36 (1987) 1527;
S. Arora, A. Buka, P. Palffy-Muhoray and Z. Racz, preprint.

[35] J. Nittman, G. Daccord and H.E. Stanley, Nature 314 (1985).
G. Daccord, J. Nittman and H.E. Stanley, Phys. Rev. Lett. 56 (1986) 336.
G. Daccord and R. Lenormand, Nature 41 (1987).

[36] K.J. Maløy, J. Feder and J. Jossang, Phys. Rev. Lett. 55 (1985) 2681.
J. Chen and D. Wilkinson, Phys. Rev. Lett. 55 (1985) 1892.

[37] D. Grier, D.A. Kessler and L.M. Sander, Phys. Rev. Lett. 59 (1987) 2315.

[38] P. Garik, D. Barkey, E. Ben-Jacob, E. Bochner, N. Broxholm, [illegible] and R. Trivedi, Phys. Rev. [illegible], in press.

[39] S.K. Chan, H.H. Reimer and M. Kahlweit, J. Cryst. Growth 32 (1976) 303.

[40] Y. Couder, O. Cardoso, D. Dupuy, P. Tavernier and W. Thom, Europhys. Lett. 2 (1986) 437.
Y. Couder, N. Gerard and M. Rabaud, Phys. Rev. A 34 (1986) 5175.
S. Zocchi, B.E. Shaw, A. Libchaber and L.P. Kadanoff, Phys. Rev. A 36 (1987) 1894.

[41] D.A. Kessler, J. Koplik and H. Levine, Phys. Rev. A 30 (1984) 316.

[42] E. Ben-Jacob, N.D. Goldenfeld, B.G. Kotliar and J.S. Langer, Phys. Rev. Lett. 53 (1984) 2110.

[43] D. Meiron, Phys. Rev. A 33 (1986) 2704;
D. Kessler, J. Koplik and H. Levine, Phys. Rev. A 33 (1986) 3352;
M. Ben Amar and B. Moussallam, Physica D 25 (1987) 155.

[44] B.I. Shraiman, Phys. Rev. Lett. 56 (1986) 2028;
D.C. Hong and J.S. Langer, Phys. Rev. Lett. 56 (1986) 2032; Phys. Rev. A 36 (1987) 2325;
R. Combescot, T. Dombre, V. Hakim, Y. Pomeau and A. Pumir, Phys. Rev. Lett. 56 (1986) 2036; Phys. Rev. A 37 (1988) 1270;
S. Tanveer, Phys. Fluids 30 (1987) 1589.
A.T. Dorsey and O. Martin, Phys. Rev. A 35 (1987) 3989;
P. Pelce and A. Pumir, J. Cryst. Growth 73 (1985) 337.

[45] A. Barbieri, D.C. Hong and J.S. Langer, Phys. Rev. A 35 (1984) 1802.
G.A. Brener, S.V. Iordanskii and V.I. Melnikov, JETP 9 (1988).
M. Kruskal and H. Segur, Aeronautical Research Associates of Princeton, Technical Memo. 85-25 (1985), unpublished;
B. Caroli, C. Caroli, B. Roulet and J.S. Langer, Phys. Rev. A 33 (1986) 442.
P. Pelce and Y. Pomeau, Stud. Appl. Math. 74 (1986) 245.

[46] Y. Saito, G. Goldbeck-Wood and H. Muller-Krumbhaar, Phys. Rev. Lett. 58 (1987) 1541.

[47] A. Dougherty, P.D. Kaplan and J.P. Gollub, Phys. Rev. Lett. 58 (1987) 652.
A. Dougherty and J.P. Gollub, Phys. Rev. A 38 (1988) 3043.

[48] R. Pieters and J.S. Langer, Phys. Rev. Lett. 56 (1987) 1948;
M. Barber, A. Barbieri and J.S. Langer, Phys. Rev. A 36 (1987) 3340.
D.A. Kessler and H. Levine, Phys. Rev. A 36 (1987) 4123.
O. Martin and N. Goldenfeld, Phys. Rev. A 35 (1987) 1382.
R. Pieters, Phys. Rev. A 37 (1988) 3126.
J.S. Langer, Phys. Rev. A 36 (1987) 3350.
D.A. Kessler and H. Levine, Phys. Rev. A 33 (1986) 2621, 2634.

[49] J.S. Langer, Science 243 (1989) 1150.

[50] N. Hecker, Senior Thesis, University of Michigan (1988).